

# An Investigation on Machining General Size Cylindrical Parts Using WEDM with Contour Approximation Method

Huliang Ma (✉ [mhl364@163.com](mailto:mhl364@163.com))

Taiyuan University of Technology

Yanqing Wang

Taiyuan University of Technology

Ming Lv

Taiyuan University of Technology

Shengqiang Yang

Taiyuan University of Technology

---

## Research Article

**Keywords:** WEDM, General Size Cylindrical Parts, Contour Approximation Method, Sequential cut, Multiple edge cut

**Posted Date:** June 30th, 2021

**DOI:** <https://doi.org/10.21203/rs.3.rs-652386/v1>

**License:**  This work is licensed under a Creative Commons Attribution 4.0 International License.

[Read Full License](#)

---

# An investigation on machining general size cylindrical parts using WEDM with contour approximation method

## Authors:

Huliang Ma, Yanqing Wang, Ming Lv, Shengqiang Yang

## Author AFFILIATIONS

School of Mechanical and Vehicle Engineering, Taiyuan University of Technology, Taiyuan, 030024, China

## Corresponding author information:

**Name:**Huliang Ma

**Email address:** [mh1364@163.com](mailto:mh1364@163.com) /[mahuliang0006@link.tyut.edu.cn](mailto:mahuliang0006@link.tyut.edu.cn)

**Telephone:**86-18291822103

**ORCID:** 0000-0002-7105-6330

## Abstract

The application of wire EDM to the machining of cylindrical parts is an emerging research topic. The current research is mainly focused on the machining of micro-cylindrical parts, and there is little research on the general-sized parts. This paper proposes to apply the principle of contour approximation method to the machining of cylindrical parts of general size. First, the basic principle of the contour approximation method is introduced, and the machining process is divided into three parts: roughing, semi-finishing and finishing. Roughing corresponds to polygon cutting. Second, the various indicators of polygon cutting are analyzed. The influence of the number of polygonal sides on the residual height and residual area is analyzed. Two methods are proposed for polygon cutting: sequential cutting and multiple edge cutting. The calculation formulas for the processing volume of the two methods are deduced. By comparing the two methods, it is found that different methods are applicable to different part sizes. At last, machining experiments were carried out. The selection of residual variables and the determination of polygon machining methods are detailed. The process parameters and machining time of each stage are listed. In addition, the measurement results of each stage of the machining are also analyzed.

**Keywords** WEDM· General Size Cylindrical Parts· Contour Approximation Method· Sequential cut· Multiple edge cut

# An investigation on machining general size cylindrical parts using WEDM with contour approximation method

## 1. Introduction

Wire electrical discharge machining (WEDM) has been widely used as a machining method for high-hardness and difficult-to-machine metal parts. Because WEDM belongs to non-contact machining, it also has unique advantages in the field of microfabrication. The use of WEDM to process micro grooves and micro cavities is also a recognized and effective method. In recent years, scholars extended the machining range of WEDM to cylindrical parts, and made some progress.

Some researchers call the method of using WEDM to process cylindrical parts as WEDT (wire electrical discharge turning). M.J. Haddad and A. Fadaei Tehrani [1-3] studied the influence of different process parameters on WEDT machining results. The machining results include surface roughness, roundness and material removal rate. This provides a reference for the estimated results of WEDT processing. E. Uhlmann [4] supplied an overview of kinematic and technological restrictions and requirements of the WEDG process influencing the process behavior with respect to the technological requirements of micromachining. V. Janardhan and G.L. Samuel [5] developed a pulse discrimination algorithm for classifying the discharge pulses during the WEDT process. The paper also revealed the changes of the discharge state under different processing conditions through experiments. Eduardo Weingärtner [6] conducted a series of single discharge experiments on workpieces with different rotation speeds to observe the shape and size of the erosion pits. The authors found that the volume of erosion pits increases with the relative velocity, which indicates that the higher the relative velocity, the higher the melting efficiency. In order to improve the processing efficiency of WEDT, A. Mohammadi [7] introduced ultrasonic vibration into the processing and conducted process experimental research. In order to optimize the material removal rate and surface roughness of WEDT, Aravind Krishnan [8] uses an artificial neural network with a feedforward backpropagation algorithm and an adaptive neuro-fuzzy inference system to model the WEDT process. The orthogonal experiment was used to train the model, and the optimization results proved that the model can improve the performance of the WEDT process. Abimannan Giridharan [9] used the finite element method (FEM) to simulate the craters with different plasma washing efficiencies in WEDT and verified them with experiments. Yingmou Zhu [10] proposed a combined feed strategy to improve the efficiency of machining long aspect ratio micro rotary parts.

Yao Sun and Yadong Gong conducted a series of researches on LS-WEDT (low-speed wire-cut electric discharge turning) machining of micro rotary parts. In the literature [11], a multi-cutting process is used to process rotary parts. In the literature [12,13,14], the processing of micro-electrodes, micro-rotating parts, spiral micro-electrodes and micro-cutting workpieces was carried out. In the literature [15,16], the machining accuracy, surface quality and machinability of micro-rotary parts are studied.

Xiang Chen [17] used fine reciprocating wire EDM to machine fine rotating

structures, and adopted multiple cutting strategies. The paper carried out the experiments of single factor design and response center compound design (CCD) plan and analyzed the results, and obtained the influence law of each factor on processing. M. Vignesh [18] tried to process Ti-6Al-4V material using diffusion annealing galvanized brass wire in WEDHT (Wire electrical discharge hybrid turning). On comparison, diffusion annealed zinc-coated brass wires outperformed uncoated brass wires with 18.95% and 44.37% for surface roughness and material removal rate criteria, respectively. Jees George [19] used the TLBO (Teaching learningbased optimization) method to optimize the roundness, cylindricity and surface roughness of Inconel 825 in multi-objective optimization in the WEDT process. In addition, the author [20] proposes a calculation technique that uses the time integration effect to simulate the crater formed in the Inconel 825 WEDT process. The average absolute errors of the single-spark experimental verification results of the proposed model and the depth and radius are 9.81% and 8.33%, respectively. In addition, the proposed model can determine the 3D surface roughness of the turned specimens. Sibabrata Mondal [21] conducted a study on the use of wire discharge turning technology to form the smallest cylindrical geometry on the electrolytic tough pitch copper (ETP Cu) material. T. Bergs [22] proposed a new method to test the load capacity of gears manufactured by WEDT. Biplab Kumar Roy [23] introduces a new method of WEDT with inclined electrode wire, which is used to process NiTi-60 shape memory alloy. This method can improve the material removal rate for specific processing objects. Pouyan Talebizadehsardari [24] studied how WEDT factors affect the surface integrity of Inconel 718 and the subsequent fatigue life and the optimization of the trade-off between productivity and fatigue life.

Additionally Yingmou Zhu [25] proposes a rapid contour approaching wire electrical discharge machining (RCA-WEDM) method based on polygon sectional feeding strategy to achieve large aspect-ratio rotational parts with high efficiency. Many of the rotational parts are made of difficult-to-cut material to achieve high performance such as superalloy material used in feedback rod and wear-resistant material used in injector plunger, which make them difficult to be machined by traditional processes. In order to fabricate those parts, the RCA-WEDM method provides a new and effective feeding strategy and approach to achieve high efficiency.

Based on the above statement, the objects of the cylindrical parts processed by WEDM are concentrated in microelectrodes and microstructures. These parts have a small machining removal volume or a large aspect ratio, and are easily deformed using traditional processing. Therefore, the WEDM method has advantages. But for cylindrical parts of general size, the amount of material removal is relatively large, and it is difficult for WEDM to have an advantage. The RCA-WEDM provides a new solution. The principle of contour approximation can be applied to the machining of cylindrical parts of general size. In this paper, it is called WEDM with contour approximation method (CAM-WEDM).

The focus of this paper is to machine general-size cylindrical parts based on CAM-WEDM. The remaining sections of the thesis are as follows: first, the principle and steps of the contour approximation method for machining cylindrical parts are

introduced. After that, the polygon contour machining was optimized, and the applicable scope and characteristics of different methods were compared. In addition, machining experiments were carried out on specific parts, and the machining process and results were explained and analyzed.

## 2. Contour approximation process

Cylindrical parts usually keep rotating during machining, and the wire electrode achieves the purpose of forming through path movement. Depending on the position of the rotation axis of the cylindrical part, WEDM has two machining methods, as shown in Figure 1.

**Fig. 1** Two types of using WEDM to process cylindrical parts

In Figure 1(a), the part rotation axis is parallel to the wire electrode, and the outermost part contour can be processed, but the remaining part cannot be machined. In Figure 1(b), the rotation axis of the part is perpendicular to the wire electrode, and the part can be machined at any position. Therefore, the use of WEDM to machine cylindrical parts refers to the second method.

When using the second method to process general-sized cylindrical parts, if the workpiece is machined while the workpiece is rotating, the amount of removal is very large. This leads to long machining time and high wire consumption. Therefore, a method is needed to quickly remove most of the material. It is proposed to use the contour approximation method to meet the requirements.

### 2.1 Process principle

The basic idea to improve the machining efficiency of cylindrical parts is to use various methods to reduce the amount of direct removal. The principle of the contour approximation method is to first keep the workpiece stationary and use a polygon to approximate the rotation diameter. The specific method is to first machine the shape of the workpiece into a regular polygon through multiple rotations, and then rotate the workpiece to remove the remaining material. The machining principle is shown in Figure 2.

**Fig. 2** Principle of contour approximation method

The process of cutting polygons is divided into three stages: rough machining, semi-finishing and finishing. During rough machining, the workpiece is stationary, and the corresponding shape is cut every time it rotates a certain angle. The stage belongs to contour machining, and there is no need to remove all the amount, which can greatly reduce the machining amount of the cylindrical part. The result of rough machining should ensure that most of the processed material is removed. This can ensure the efficiency of finishing.

### 2.2 Machining steps

Compared with LS-WEDM, MS-WEDM is more economical to machine general-size cylindrical parts because the wire electrode can be reused. At different stages of the general size of cylindrical parts, the concerns are as follows:

(1) Roughing. The workpiece is stationary during machining, and the machine tool moves to cut off the specified shape. The workpiece rotates by a certain angle and runs the same path again. Repeat this process until the polygon is shaped. When this step is completed, most of the machining volume is removed.

(2) Semi-finishing. The workpiece rotates at a low speed while the wire electrode feeds at a low speed, and the machining path is cycled multiple times. After several times of machining, gradually increase the speed of the workpiece to ensure the machining efficiency. When this step is completed, the edges and corners of the polygon disappear and the workpiece contour becomes a cylinder.

(3) Finishing. The workpiece keeps high-speed rotation, the wire electrode is fed at a low speed, and the process parameters are adjusted at the same time to reduce the amount of erosion and achieve the workpiece machining accuracy.

The flowchart corresponding to the machining steps is shown in Figure 3:

**Fig. 3** Flow chart of machining general size cylindrical parts by wire EDM

The purpose of rough machining is high-efficiency machining. Therefore, the process parameters with a large amount of erosion and the high-speed servo strategy are adopted to shorten the machining time as much as possible. Since the workpiece is in the rough machining stage, which is the same as the traditional machining method, the parameters can be set with reference to the existing process database.

In semi-finish machining, the workpiece is rotated and the removed material is distributed on the circumferential dimension of the workpiece. Therefore, the wire electrode is set to feed at a low speed to ensure machining to all positions. Low-speed rotation of the workpiece is discovered through actual machining. The machining current during low-speed rotation is larger than that of high-speed rotation, so the material removal rate (MRR) is higher. Therefore, semi-finishing chooses large current, large pulse width, low-speed wire feed and low-speed rotation of the workpiece.

During the finishing process, due to the small amount of erosion, in order to improve the accuracy, the running speed of the wire can be reduced, and the pulse width and current can be reduced at the same time.

### **2.3 Process improvement method**

In the process of contour approximation method, the first step is the part with the largest amount of erosion and the longest time consuming. Therefore, the optimization analysis of the first step is one of the effective ways to improve the machining efficiency.

The first step is polygon cutting. The number of sides of different polygons and the machining order of these sides affect the amount of removal, which is a problem that needs to be studied.

The optimization of the second and third steps is mainly achieved through the adjustment of process parameters.

### 3 Polygon machining optimization

#### 3.1 Determination of the number of polygon sides

Determining the number of sides is the first step in machining a polygon. The more sides of a regular polygon, the closer it is to a circle. A regular polygon is usually selected as the closest approximation to the contour.

##### 3.1.1 Calculation of residual parameters

After the polygon is machined, the workpiece contour will have periodic size fluctuations, as shown in Figure 4(a). The difference between the maximum value and the minimum value of the size fluctuation is called the residual height  $\Delta h$ . The residual height calculation formula is as follows:

$$\Delta h = l - r = r \cdot [1/\cos(\alpha/2) - 1] \quad (1)$$

where  $l$  represents the radius of the circumcircle of the polygon,  $r$  represents the radius of the target circle, and  $\alpha$  represents the center angle of the polygon.

**Fig. 4** Definition of (a) residual height  $\Delta h$  (b) residual area  $\Delta A$

The difference between the area of the machined polygon and the area of the target circle is called the residual area  $\Delta A$ , and the corresponding volume is called the residual volume  $\Delta V$ . As shown in Figure 4(b),  $S_{pol}$  represents the area of the polygon,  $S_{aim}$  represents the area of the target circle,  $S_{raw}$  represents the area of the raw workpiece,  $\Delta S$  represents the area difference between the original workpiece and the polygon. The formula for calculating the residual area is as follows:

$$\Delta A = S_{pol} - S_{aim} = [N \cdot \tan(180/N) - \pi] \cdot r^2 \quad (2)$$

where  $N$  represents the number of polygon sides. For regular polygons,  $\alpha = 360/N$ .

According to formula 1 and formula 2, the more polygon sides, the smaller the residual height and residual area, which can reduce the amount of semi-finishing removal. Therefore, the number of polygonal sides needs to ensure that the amount of machining in the second step is within a reasonable range.

##### 3.1.2 Influence of the number of polygon sides

The number of polygon sides is determined by the residual, and the relationship between the number of sides  $N$  and the residual height  $\Delta h$  is shown in Figure 5(a). The relationship between the number of sides  $N$  and the residual area  $\Delta A$  is shown in Figure 5(b). The corresponding values in Figure 5 are shown in Table 1.

It can be seen from Table 1 and Figure 5 that when the size of the workpiece is large and the number of sides is small, the residual height and residual area are very large. For different sizes, when  $N$  is greater than a certain value, the residual changes tend to be flat. At this time, the reduction of the residual height is of little significance. Therefore, the number of the polygon sides is not that more is better. Instead, a more suitable number of sides should be selected according to the size of the workpiece and the residual error.

**Table 1** Residual indicators of polygon cutting

**Fig. 5** The relationship between the number of polygon sides and

(a) the residual height  $\Delta h$  (b) the residual area  $\Delta A$

### 3.2 Calculation of sequential cutting method

After the number of the polygon sides is determined, it is necessary to determine the machining order of the polygon. There are two methods for machining polygons in different orders. This section introduces the first method.

The conventional method is the sequential cut method. Each time the workpiece rotates, the angle is determined, and each side of the polygon is cut out in turn. This method has a clear sequence and simple operation, but it has a large amount of machining. Since the length of each cut is one more than the length of a single side of the polygon, there is a certain amount of excess cutting. In the octagon shown in Figure 6, the cutting sequence is  $L_1$  to  $L_8$ , where  $L_1$  to  $L_7$  all contain excess cutting amount, and  $L_8$  has no excess cutting amount.

Fig. 6 Schematic diagram of sequential cutting

Through analysis, there are three cases for the machining area of the sequential cut method, as shown in Figure 7. Take the octagon as an example. Since  $L_1$  does not interfere with other sides, it belongs to a single situation.  $L_2 \sim L_6$  is the second case, these cuts only interfere with the previous one.  $L_7$  and  $L_8$  is the third case, which interferes with the first and previous cuts. If the number of polygon sides increases, the number of the second and third cases will also increase. The calculation of the side length in the three cases is shown in Figure 7.

Fig. 7 Cutting length calculation (a) the first case (b) the second case (c) the third case

The calculation formula for the machining length of the sequential cutting method is as follows

$$L_n = \begin{cases} 2\sqrt{R^2 - r^2} & , & n = 1 \\ r \cdot \tan(\alpha/2) + \sqrt{R^2 - r^2} & 1 < n \leq N_\beta \\ r \cdot \tan(\alpha/2) + r \cdot \tan\gamma & N_\beta < n \leq N \end{cases} \quad (3)$$

where  $R$  represents the diameter of the raw outline,  $\beta$  represents half of the central angle of the first cut,  $\beta = \arccos(r/R)$ ,  $\gamma$  represents the calculation auxiliary angle in the third case,  $\gamma = (N - n + 1)\alpha/2$ ,  $N_\beta$  represents the number of the second case,  $N_\beta = (360^\circ - \beta)/\alpha$ , and  $n$  represents the serial number of the current side.  $N$  and  $N_\beta$  are integers. After calculating the length of each cutting, the machining area is calculated as follows

$$A = H \cdot \sum_{n=1}^N L_n \quad (4)$$

where  $H$  represents the thickness of the workpiece.

### 3.3. Calculation of multiple cutting method

This section introduces the second method of polygon cutting. Another method is called the multiple edge cutting method. Form a polygon with a smaller number of sides first, and then double the number of sides to increase the number of polygons. The multiple edge cutting method determines the name according to the specific multiple value. For example, the double cutting method indicates the multiple once,

and the triple method indicates the multiple twice. Specifically, the double cutting method first cuts the shape of the workpiece into an N/2-sided shape, and then cuts two adjacent sides to obtain a N-sided shape.

The cutting sequence of multiple method is shown in Figure 8, first cut into a 4-sided shape, and then cut into 8 deformation. This method also has excess resection. There are excess cutting amounts from L1 to L4, and no excess cutting amounts from L5 to L8.

**Fig. 8** Schematic diagram of multiple edge cutting method

The cutting area of the multiple cutting method is different from the sequential cutting method. The cutting amounts are based on the value of the multiple. Taking the triple method as an example, there are three situations. Assuming that the number of sides of the final polygon is N, the cutting order of the triple method is N/4, N/2 to N. The calculation of side length is as follows:

(1) Calculation of N/4 polygon. Since it is the first cut, it is related to the shape of the raw outline.  $\alpha_{N/4}$  represents the center angle of the N/4 polygon. When  $\alpha_{N/4} < 2\beta$ , the front and rear cutting lines cross, as shown in Figure 9(a), when  $\alpha_{N/4} > 2\beta$ , the front and rear blades are separated from each other, as shown in Figure 9(b). The two cases use different formulas when calculating the cutting length:

$$L_{N/4} = \begin{cases} \sum_{n=1}^{N/4} L_n & \alpha_{N/4} < 2\beta \\ \frac{N}{2} \cdot \sqrt{R^2 - r^2} & \alpha_{N/4} > 2\beta \end{cases} \quad (5)$$

**Fig. 9** Cutting length calculation (a)  $L_{N/4}$  when  $\alpha_{N/4} \leq 2\beta$  (b)  $L_{N/4}$  when  $\alpha_{N/4} \geq 2\beta$

(2) Calculation of N/2 polygon. Usually when N/2 polygonal machining is performed, due to the large number of sides, it has nothing to do with the dimensions of the raw workpiece.  $\alpha_{N/2}$  represents the center angle of the N/2-sided polygon. As shown in Figure 10(a), the cutting size of N/2 is calculated as follows

$$L_{N/2} = r \times \tan(\alpha_{N/2}/2) \cdot N/2 \quad (6)$$

(3) Calculation of N polygon. This is the third step of polygon cutting to obtain a polygon with N sides.  $\alpha_N$  represents the center angle of the N-sided polygon. As shown in Figure 10(b), the cutting length of N/2 is calculated as follows

$$L_N = r \times \tan(\alpha_N/2) \cdot N \quad (7)$$

**Fig. 10** Cutting length calculation (a)  $L_{N/2}$  (b)  $L_N$

The polygon cutting area of the triple cutting method is calculated as follows

$$A = H \cdot (L_{N/4} + L_{N/2} + L_N) \quad (8)$$

According to the calculation formula of the triple cutting method, the double cutting method and the quadruple cutting method can be derived. Because of the multiple edge cutting method, the number of polygon sides must be an integer. The polygon side number N of the double cutting method must be a multiple of 2. The number of sides N of the triple cutting method must be a multiple of 4. The number of sides N of the quadruple cutting method must be a multiple of 8. If the multiple is too

large, it is not conducive to the selection of the number of polygon sides. Therefore, the double method, triple method and quadruple method can be actually used for the multiple cutting method.

### 3.4 Comparison of the two methods

The area  $\Delta S$  removed by the two methods is equal in the roughing, but the machining area  $A$  is not equal, and there is a certain amount of excess cutting. This section calculates and compares the two cutting methods.

#### 3.4.1 Comparison of machining area

When the diameter  $D$  of the raw workpiece is 70mm, the diameter  $d$  to be machined is 60mm, and the thickness of the workpiece  $H$  is 10mm, the change trend of the machining area with the number of sides is shown in Table 2 and Figure 11. The effective area refers to the product of the side length and the thickness of a polygon. The larger the number of sides, the closer the effective area is to the cylindrical side area. When the number of sides is small, the difference between the machining areas of the two machining methods is smaller, and the more the number of sides, the greater the difference. The machining area of the sequential cutting method increases with the increase of the number of sides  $N$ . This is because each cut in the sequential cutting method cuts the outer contour, which causes more redundancy. In contrast, the cutting area of the multiple edge cutting method becomes smaller because only the first cutting has excess cutting. Therefore, the multiple cutting method has higher cutting machining efficiency. By comparison, the cutting area of triple cutting method is the smallest. Therefore, for the current size, the triple cutting method should be selected for polygon machining.

**Table 2** Comparison of different methods of the same size ( $D=70\text{mm}$ ,  $d=60\text{mm}$ ,  $H=10\text{mm}$ )

**Fig. 11** The relationship between the number of polygon sides and machining area

For the same size, the more polygonal sides, the larger the machining area of the two polygon cutting methods. The sequential cutting method grows faster, and the multiple edge cutting method grows slowly. When the triple cutting method is deformed at 24, the cutting area suddenly becomes smaller because the  $N/4$  sets of cutting sizes occur interference. Among them, the reduction of angle  $\alpha_{N/4}$  causes the calculation of the cutting length to change, please refer to formula 5.

#### 3.4.2 The influence of target size

When the polygon side number  $N$  is 32, the change rule of the machining area with the diameter under different target diameters is shown in Figure 12. The machining area of the two methods increases with the increase of the diameter. However, the machining area of the multiple edge cutting method is smaller than that of the sequential cutting method.

**Table 3** Comparison of different methods with the same number of sides ( $N=32$ ,  $H=10\text{mm}$ )

**Fig. 12** The influence of target size on machining area

Therefore, the use of multiple method for roughing can reduce the machining area and improve the machining efficiency. According to the Table 3 and Figure 12, when  $N=32$ , the smaller the target size, the smaller the machining area. When the target size increases, the sequential cutting method increases faster, and the multiple cutting method increases slowly. At the same time, when  $d < 30\text{mm}$ , the area of the quadruple cutting method is the smallest, and when  $d > 30\text{mm}$ , the area of the triple cutting method is the smallest.

In summary, the multiple edge cutting method has a smaller cutting area than the sequential cutting method. The selection of the specific multiple cutting method needs to be calculated according to the actual situation, and the method with the smallest processing area is selected.

## **4. Processing Experiment**

This section uses machining experiments to illustrate the application of the contour approximation method.

### **4.1 Experimental platform and machining object**

The experiment is based on the MS-WEDM machine tool, the model is DK7732ZAA. The spindle rotating platform is built on it as shown in Figure 13. The spindle is driven by a stepping motor through a synchronous belt. The workpiece is fixed by a three-jaw chuck on the spindle. The rotation angle and speed are controlled by the motor driver. The spindle is connected to the pulse power supply through the graphite block.

The machining object of this experiment is the titanium alloy TC4. TC4 titanium alloy has a series of advantages such as excellent corrosion resistance, small density, high specific strength, better toughness and weldability, etc. It has been successfully applied in aerospace, petrochemical, shipbuilding, automotive, pharmaceutical and other sectors.

The machining requirements of the outer circle and groove of the workpiece are shown in Figure 14. The diameter of the raw workpiece is 70mm, the target diameter is 60mm and it contains three grooves with a width of 1mm. This workpiece is suitable for WEDM with contour approximation method.

**Fig. 13** Cylindrical parts machining platform

**Fig. 14** Dimensions of (a) raw part (b) processed part

## **4.2. Experimental process arrangement**

### **4.2.1 Determination of residual height**

After the machining size is determined, the number of sides  $N$  during rough machining needs to be determined by determining the residual error. In the exploration stage, experiments were conducted with multiple residual values to observe the influence of different residual values on subsequent processing.

As shown in Figure 15, when the residual height  $\Delta h \leq \tau_{\text{kerf}}$ , only a single path needs to be generated for machining. When the residual height  $\Delta h > \tau_{\text{kerf}}$ , it is necessary to form a multi-layer path.  $\tau_{\text{kerf}}$  represents the kerf width of the wire electrode. The value of the kerf width is related to the size of the wire electrode, the discharge gap and the feed speed and other parameters, so it is difficult to calculate. The kerf width observed through actual machining is about 0.3mm.

**Fig. 15** Countermeasures for residual height

The exploratory experiments prove that when  $\Delta h > 0.3\text{mm}$ , the polygon edge removal efficiency is significantly reduced. The reason is that there are a lot of materials to be removed. At the same time, when the workpiece is rotating, it is not guaranteed that every edge can be machined, so multiple machining is required to achieve the effect of eliminating the edge. When the workpiece is rotating, the current changes greatly, and there are many short-circuit states during machining, which is not conducive to subsequent machining.

When  $\Delta h \leq 0.3\text{mm}$ , less material needs to be removed and machining is smoother. Therefore, in order to achieve a good machining effect, this experiment is designed with  $\Delta h \leq 0.3\text{mm}$ .

#### **4.2.2 Determination of the number of polygon sides and cutting method**

According to the analysis in Section 3.4, the cutting area of this workpiece using the triple cutting method is the smallest. The number of polygon sides that meet the triple cutting method and residual requirements are 24, 28, 32, and 36. The calculation of various indexes of the workpiece polygon cutting is shown in Table 4. Three small grooves are included in the machining size, and it is more complicated to calculate completely. The data in Table 4 is calculated using the outline dimensions of the part.

**Table 4** Various indexes of workpiece polygon cutting

From the data in Table 4, it can be seen that the cutting area of the triple cutting method only accounts for about half of the sequential cutting method. Therefore, the triple cutting method is selected to cut the polygonal outline. All three sides meet the requirements and can be selected.

#### **4.2.3 Determination of process parameters at each stage**

The process parameters selected for each stage are shown in Table 5. When rough machining, large discharge parameters are used for machining, and servo feed is used to improve machining efficiency. In semi-finishing machining, the speed of the workpiece is gradually increased to achieve the effect of eliminating edges, and the feed rate is limited to a lower value. Finish machining improves machining accuracy by adjusting discharge parameters, wire speed and so on.

**Table 5** Processing parameters of the experimental process

### **4.3 Analysis of results**

The machining time of the two methods is shown in Table 6. The machining time of

the triple cutting method is significantly shorter than that of the sequential cutting method. The machining efficiency of the triple cutting method in the roughing stage is increased by 41%, 44%, 48%, and 49%, and the total machining efficiency is increased by 32%, 37%, 42%, and 49%, respectively.

The change trend of the machining time of the two methods is shown in Figure 16. The roughing and total time of sequential cutting method increases with the increase of the number of sides. The roughing time of the triple cutting method increases with the increase of the number of sides, but the total time is decreasing, because the increased time of roughing is less than the decreased time of radius machining.

**Table 6** Machining time results

**Fig. 16** Machining time of two methods

After each stage of processing is completed, the laser displacement sensor is used to measure the radial runout, and the measurement result is shown in Figure 17. The measurement results show that the residual height  $\Delta h$  after rough machining is about  $\pm 0.2\text{mm}$ , which is consistent with the theoretical calculation value. After the semi-finishing is completed, the diameter jump is about  $\pm 25\mu\text{m}$ , indicating that the edge elimination effect is obvious, and the polygonal contour gradually tends to the circular contour. After finishing, the measured diameter jump is within  $\pm 10\mu\text{m}$ . This is because after adjusting the process parameters, the erosion amount is reduced and the machining accuracy is improved.

**Fig. 17** Data measurement in the circumferential direction (a) roughing (b) semi-finishing (c) finishing

The rotating part is shown in Figure 18. The experimental results show that as the machining progresses, the contour of the workpiece gradually approaches a circle, which verifies the feasibility of this process method. The machining discharge area appears blue-violet. This is because spark discharge releases heat to remove material, while metallic titanium is blue-violet when heated at  $600^\circ\text{C}$ .

**Fig. 18** Workpiece contour (a) online (b) completed

## 5 Conclusions

Through the improved contour approximation method, the complete method and process of wire EDM machining of cylindrical parts is obtained, and the polygon machining area calculation are completed. Finally, the effectiveness of CAM-WEDM is verified by experiments. The conclusions are as follows:

(1) The different cutting order of the polygon will affect the machining volume and thus the machining efficiency. The machining volume of the multiple edge cutting method is significantly less than that of the sequential cutting method. Choosing the appropriate multiple edge cutting method for different sizes can greatly improve the machining efficiency.

(2) When machining cylindrical parts with contour approximation method, in order to facilitate subsequent machining, it is reasonable that the residual height  $\Delta h$  after machining is less than  $0.3\text{mm}$ .

(3) In the semi-finishing stage, when removing the edges, streaks will appear on the surface of the workpiece. Need to cycle the machining path multiple times to eliminate streaks. The reduction of pulse discharge energy during finishing is conducive to the improvement of the surface quality of the workpiece.

Through experiments and analysis, the MS-WEDM can cut large-sized cylindrical parts, which has obvious advantages compared with traditional methods when machining difficult-to-process materials. In the next step, the process law of each stage of the contour approximation method will be studied, and the process parameters will be optimized to further improve the machining efficiency.

## **Acknowledgments**

This work is supported by the Shanxi Key R & D Program Project of China under grant number 201903D121048.

## **Declarations**

### **Ethical Approval:**

Not applicable. The research content of this paper does not involve any people or animals.

### **Consent to Participate:**

Not applicable.

### **Consent to Publish:**

Not applicable.

### **Authors' contributions:**

The proposal and realization of this technology were mainly completed by Huliang Ma and Yanqing Wang. Yang Shengqiang and Lv Ming provided guidance on research directions.

### **Funding:**

The sponsor is the Science and Technology Department of Shanxi Province, China, which is a general scientific research grant and does not involve any company.

### **Conflicts of interest/Competing interests:**

**Financial interests:** Author Huliang Ma and Yanqing Wang have received research support from the funding.

**Non-financial interests:** Author Shengqiang Yang and Ming Lv did not get paid from the funding.

### **Availability of data and material:**

All data generated or analysed during this study are included in this published paper.

### **Code availability:**

Not applicable.

## References

- 1 Mohammad Jafar Haddad, Alireza Fadaei Tehrani (2008) Investigation of cylindrical wire electrical discharge turning (CWEDT) of AISI D3 tool steel based on statistical analysis. *Journal of Materials Processing Technology* 98: 77–85. <https://doi.org/10.1016/j.jmatprotec.2007.06.059>
- 2 M.J. Haddad, A. Fadaei Tehrani (2008) Material removal rate (MRR) study in the cylindrical wire electrical discharge turning (CWEDT) process. *Journal of Materials Processing Technology* 199: 369–378. <https://doi.org/10.1016/j.jmatprotec.2007.08.020>
- 3 Aminollah Mohammadi, Alireza Fadaei Tehrani, Ehsan Emanian, Davoud Karimi (2008) Statistical analysis of wire electrical discharge turning on material removal rate. *Journal of Materials Processing Technology* 205: 283–289. <https://doi.org/10.1016/j.jmatprotec.2007.11.177>
- 4 E. Uhlmann, S. Piltz, D. Oberschmidt (2008) Machining of micro rotational parts by wire electrical discharge grinding. *Production Engineering-Research and Development* 2: 227–233. <https://doi.org/10.1007/s11740-008-0094-4>
- 5 V. Janardhan, G.L. Samuel (2010) Pulse train data analysis to investigate the effect of machining parameters on the performance of wire electro discharge turning (WEDT) process. *International Journal of machine tools & manufacture.* 50: 775–788. <https://doi.org/10.1016/j.ijmachtools.2010.05.008>
- 6 Eduardo Weingärtner, Konrad Wegener, Friedrich Kuster (2012) Wire electrical discharge machining applied to high-speed rotating workpieces. *Journal of Materials Processing Technology* 212: 1298–1304. <https://doi.org/10.1016/j.jmatprotec.2012.01.005>
- 7 Mohammadi A, Tehrani A F, Abdullah, A (2013) Introducing a New Technique in Wire Electrical Discharge Turning and Evaluating Ultrasonic Vibration on Material Removal Rate. *CIRP Conference on Electro Physical and Chemical Machining* 6: 583–588. <https://doi.org/10.1016/j.procir.2013.03.005>
- 8 S. Aravind Krishnan, G. L. Samuel (2013) Multi-objective optimization of material removal rate and surface roughness in wire electrical discharge turning. *Int J Adv Manuf Technol* 67: 2021–2032. <https://doi.org/10.1007/s00170-012-4628-8>
- 9 Giridharan, Abimannan, Samuel G L (2015) Modeling and analysis of crater formation during wire electrical discharge turning(WEDT) process. *The International Journal of Advanced Manufacturing Technology* 77: 1229–1247. <https://doi.org/10.1007/s00170-014-6540-x>
- 10 Zhu Yingmou, Liang Tongsheng, Gu Lin, Zhao Wansheng (2016) Machining of Micro Rotational Parts with Wire EDM Machine. *Procedia Manufacturing* 5: 849–856. <https://doi.org/10.1016/j.promfg.2016.08.071>
- 11 Sun Yao, Gong Yadong (2017) Experimental study on the microelectrodes fabrication using low speed wire electrical discharge turning (LS-WEDT) combined with multiple cutting strategy. *Journal of Materials Processing Technology* 250: 121–131. <https://doi.org/10.1016/j.jmatprotec.2017.07.015>
- 12 Sun Yao, Gong Yadong, Liu Yin, Li Qiang, Zhou Yunguang (2017) Experimental study on surface characteristics and improvement of microelectrode machined by low speed wire electrical discharge turning. *Archives of Civil and Mechanical Engineering* 17: 964–977. <https://doi.org/10.1016/j.acme.2017.02.004>
- 13 Sun Yao, Gong Yadong, Liu Yin, Cai Ming, Ma Xiaoteng, Li Pengfei (2018) Experimental investigation on effects of machining parameters on the performance of Ti-6Al-4V micro rotary parts fabricated by LS-WEDT. *Archives of Civil and Mechanical Engineering* 18: 385–400.

- <https://doi.org/10.1016/j.acme.2017.09.006>
- 14 Sun Yao, Gong Yadong (2018) Experimental study on fabricating spirals micro electrode and micro-cutting tools by low speed wire electrical discharge turning. *Journal of Materials Processing Technology* 258: 271-285. <https://doi.org/10.1016/j.jmatprotec.2018.04.007>
  - 15 Sun Yao, Gong Yadong, Ma Yongkang, Yang Yuying, Liang Chunyou (2018) An experimental study for evaluating the machining accuracy of LS-WEDT and its application in fabricating micro parts. *The International Journal of Advanced Manufacturing Technology* 98: 969–983.
  - 16 Sun Yao, Gong Yadong, Yin Guoqiang, Cai Ming, Li Pengfei (2018) Experimental study on surface quality and machinability of Ti-6Al-4V rotated parts fabricated by low-speed wire electrical discharge turning. *The International Journal of Advanced Manufacturing Technology* 95:2601–2611. <https://doi.org/10.1007/s00170-017-1360-4>
  - 17 Chen Xiang, Wang Zhenlong, Wang Yukui, Chi Guanxin, Guo Cheng (2018) Micro reciprocated wire-EDM of micro-rotating structure combined multi-cuttingstrategy. *The International Journal of Advanced Manufacturing Technology* 97: 2703–2714. <https://doi.org/10.1007/s00170-018-2145-0>
  - 18 Vignesh M, Ramanujam R (2019) Machining of Ti–6Al–4V using difusion annealed zinc-coated brass wire in WEDHT. *Journal of the Brazilian Society of Mechanical Sciences and Engineering* 41: 359. <https://doi.org/10.1007/s40430-019-1860-2>
  - 19 George Jeas, Manu R, Mathew Jose (2019) Multi-objective optimization of roundness, cylindricity and areal surface roughness of Inconel 825 using TLBO method in wire electrical discharge turning (WEDT) process. *Journal of the Brazilian Society of Mechanical Sciences and Engineering* 41: 377. <https://doi.org/10.1007/s40430-019-1880-y>
  - 20 George Jeas, Mathew Jose, Manu R (2020) Determination of Crater Morphology and 3D Surface Roughness in Wire Electrical Discharge Turning of Inconel 825. *Arabian Journal for Science and Engineering* 45:5109–5127. <https://doi.org/10.1007/s13369-020-04372-2>
  - 21 Mondal Sibabrata, Bose Dipankar (2020) Formation of smallest cylindrical geometries by wire electrical discharge turning process. *Materials Today: Proceedings* 26:1500-1506. <https://doi.org/10.1016/j.matpr.2020.02.310>
  - 22 Bergs T, Tombul U, Mevissen D, Klink A, Brimmers J (2020) Load Capacity of Rolling Contacts Manufactured by Wire EDM Turning. *Procedia CIRP* 87: 474–479. <https://doi.org/10.1016/j.procir.2020.02.111>
  - 23 Biplab Kumar Roy, Amitava Mandal (2021) An investigation into the effect of wire inclination in Wire-Electrical Discharge Turning process of NiTi-60 shape memory alloy. *Journal of Manufacturing Processes* 64: 739–749. <https://doi.org/10.1016/j.jmapro.2021.01.050>
  - 24 Talebizadehsardari Pouyan, Eyvazian Arameh, Musharavati Farayi, Zeeshan, Qasim, Mahani Roohollah Babaei, Sebaey Tamer A (2021) Optimization of wire electrical discharge turning process trade-off between production rate and fatigue life. *The International Journal of Advanced Manufacturing Technology* 112:719–730. <https://doi.org/10.1007/s00170-020-06351-1>
  - 25 Zhu Yingmou, Farhadi Ahmad, He Guojian, Liang Tongsheng, Gu Lin, Zhao Wansheng (2018) High-efficiency machining of large aspect-ratio rotational parts by rapid contour approaching WEDM. *The International Journal of Advanced Manufacturing Technology* 94:3577–3590. <https://doi.org/10.1007/s00170-017-1090-7>

## Figures

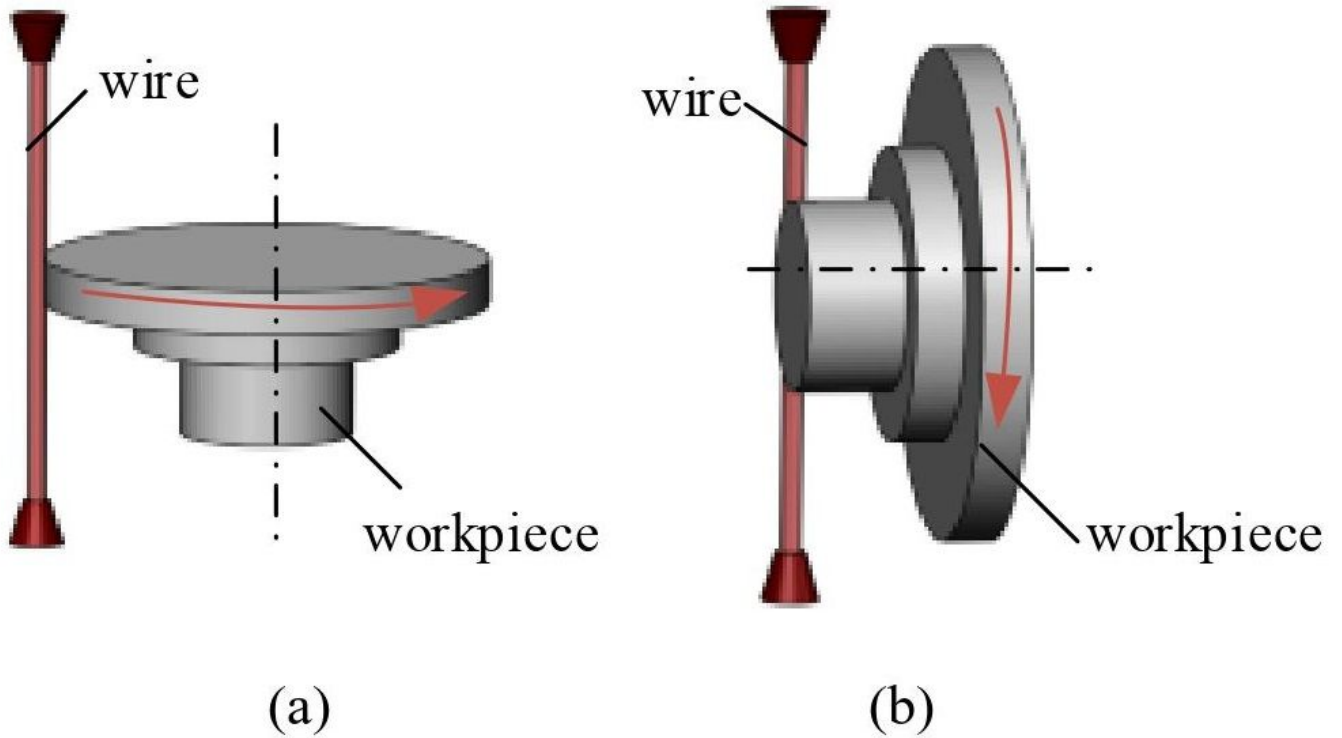


Figure 1

Two types of using WEDM to process cylindrical parts

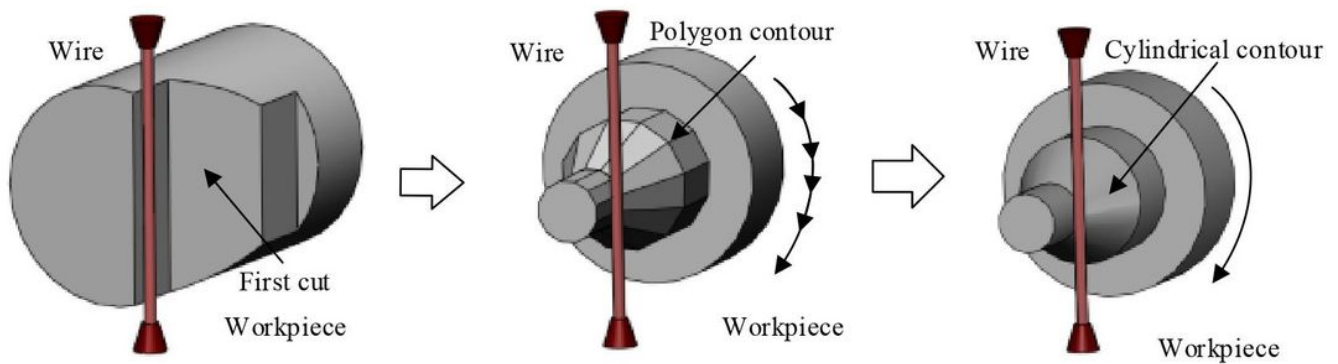


Figure 2

Principle of contour approximation method

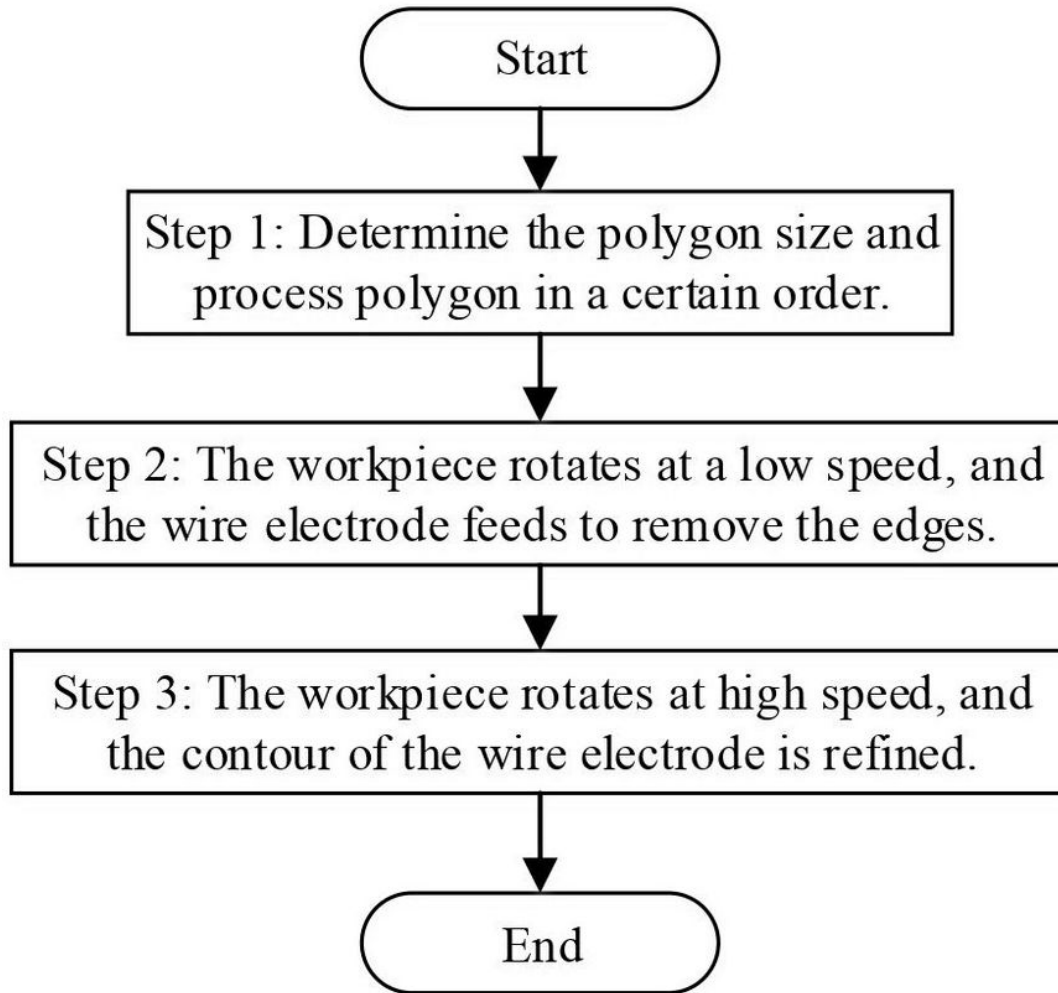


Figure 3

Flow chart of machining general size cylindrical parts by wire EDM

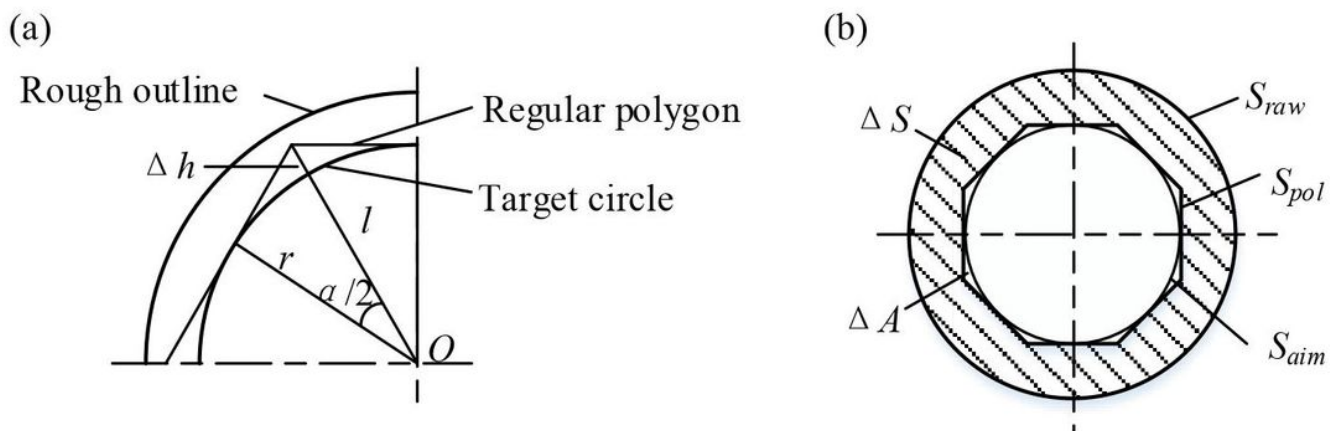
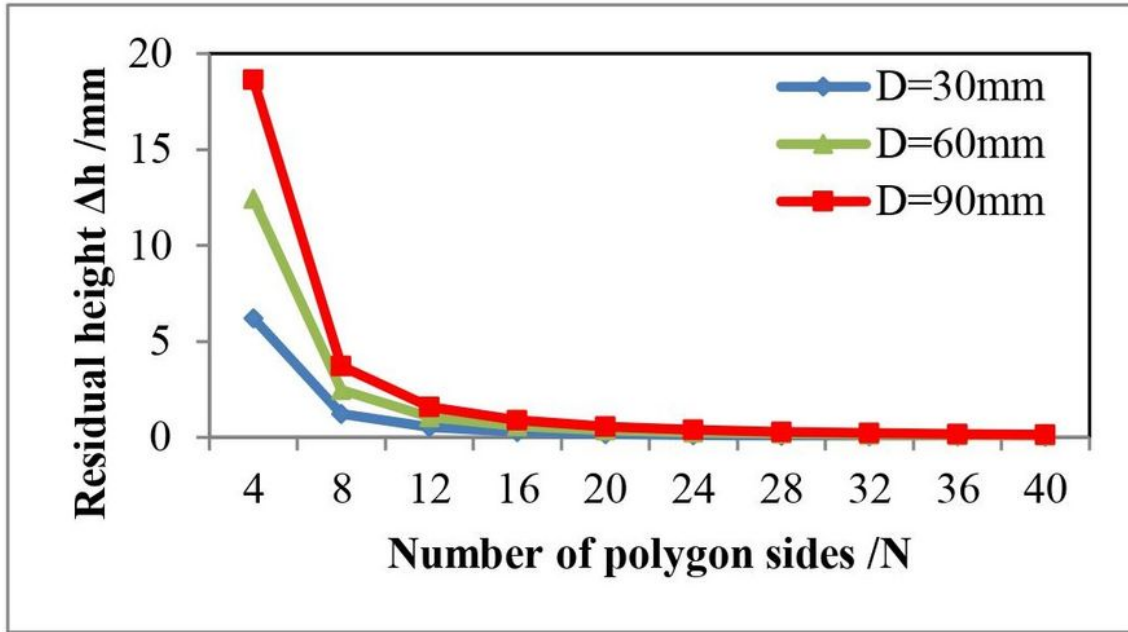
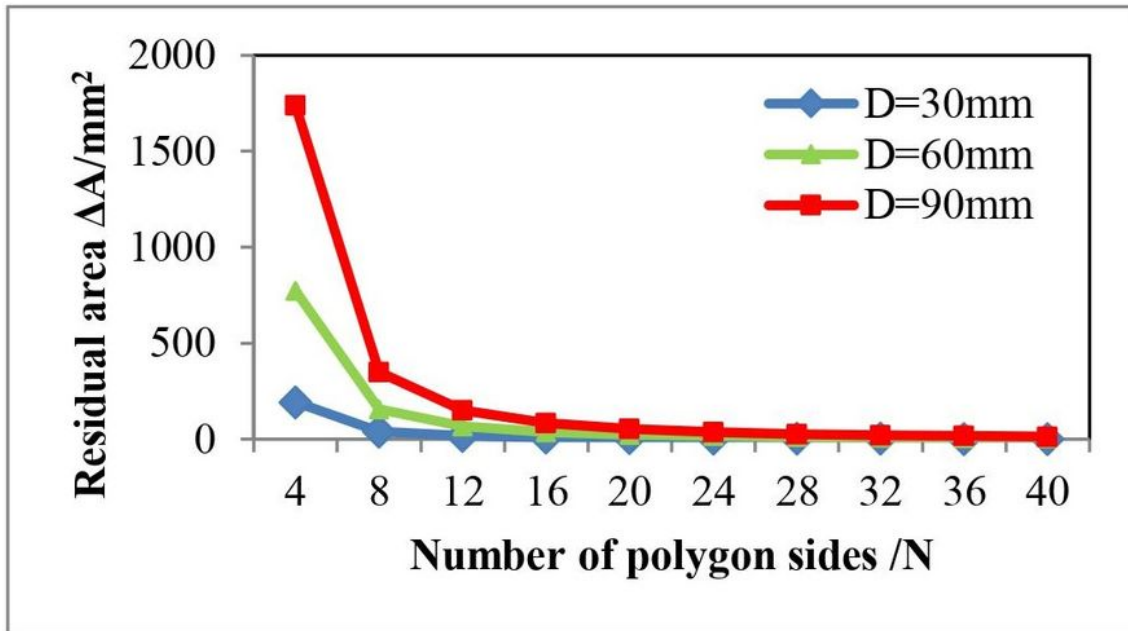


Figure 4

Definition of (a) residual height  $\Delta h$  (b) residual area  $\Delta A$



(a)



(b)

Figure 5

The relationship between the number of polygon sides and (a) the residual height  $\Delta h$  (b) the residual area  $\Delta A$

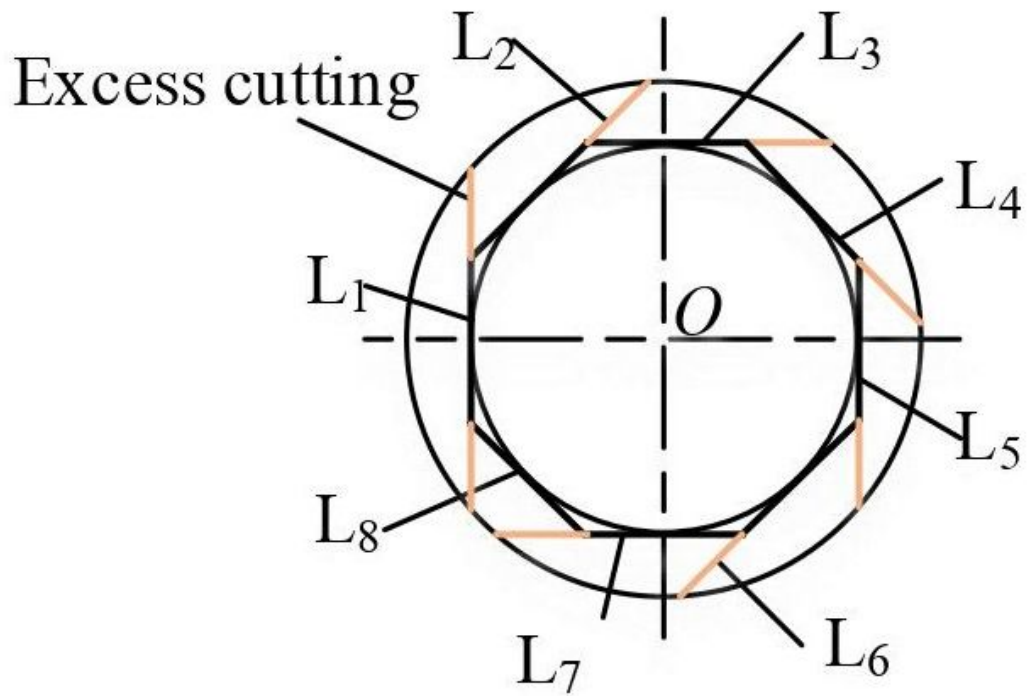


Figure 6

Schematic diagram of sequential cutting

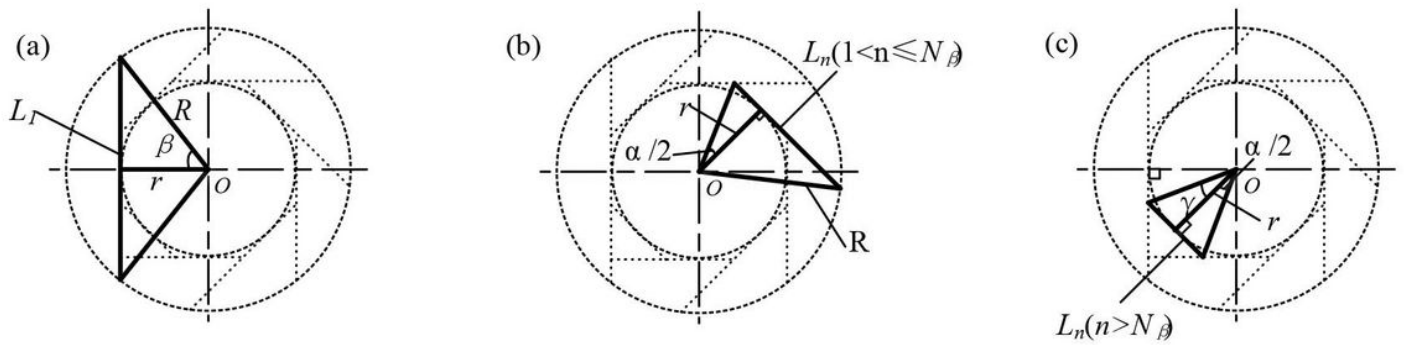


Figure 7

Cutting length calculation (a) the first case (b) the second case (c) the third case

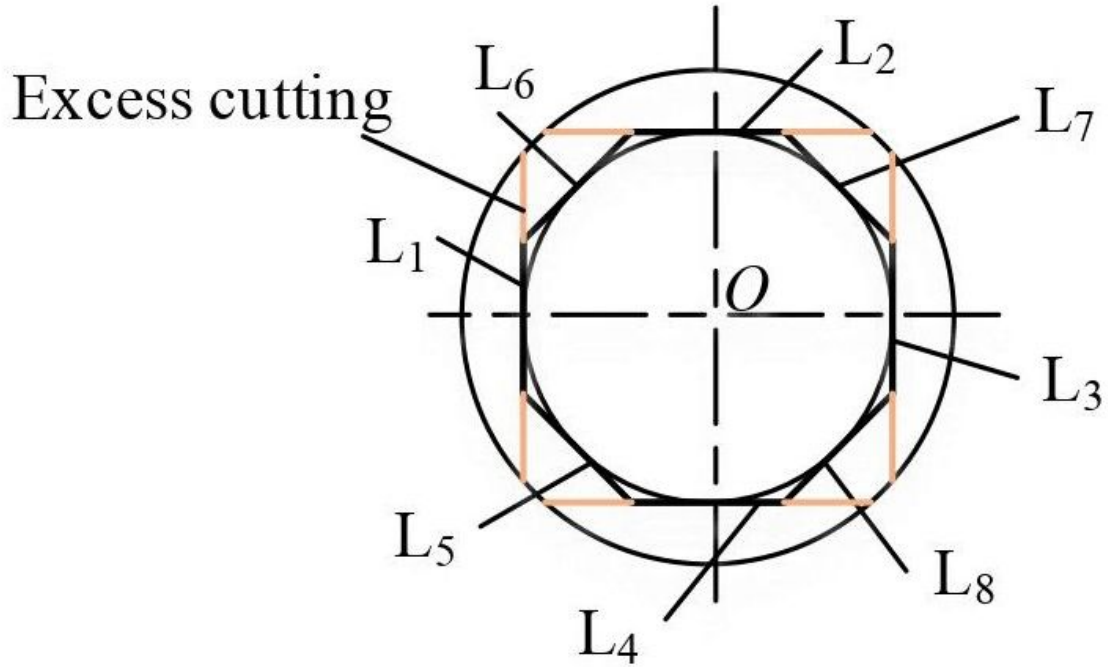


Figure 8

Schematic diagram of multiple edge cutting method

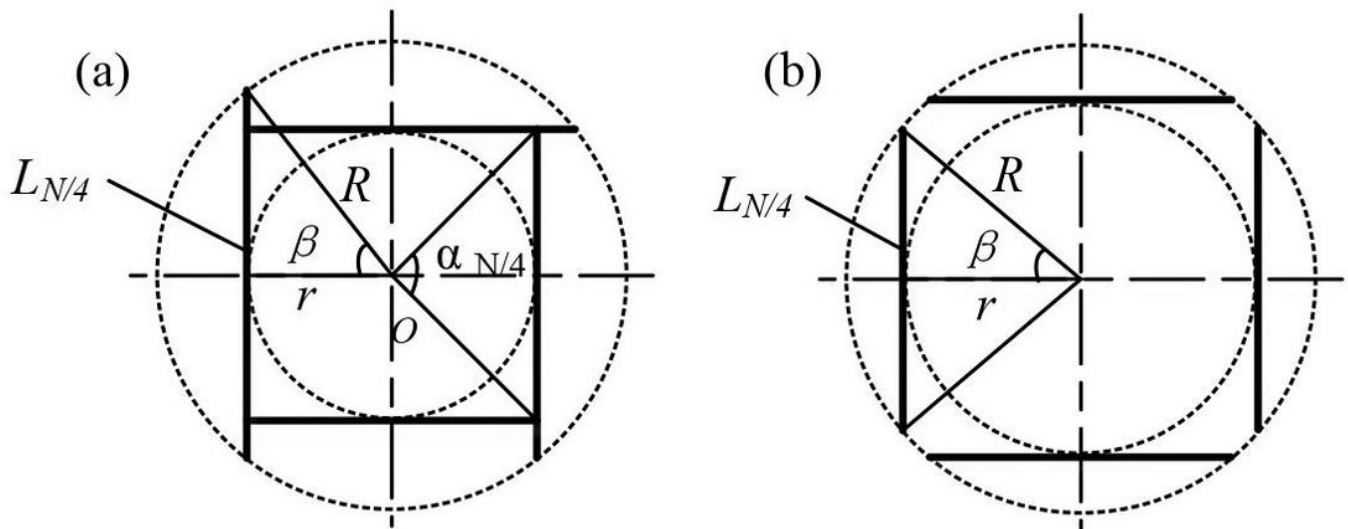


Figure 9

Cutting length calculation (a)  $L_{N/4}$  when  $\alpha_{(N/4)} \leq 2\beta$  (b)  $L_{N/4}$  when  $\alpha_{(N/4)} \geq 2\beta$

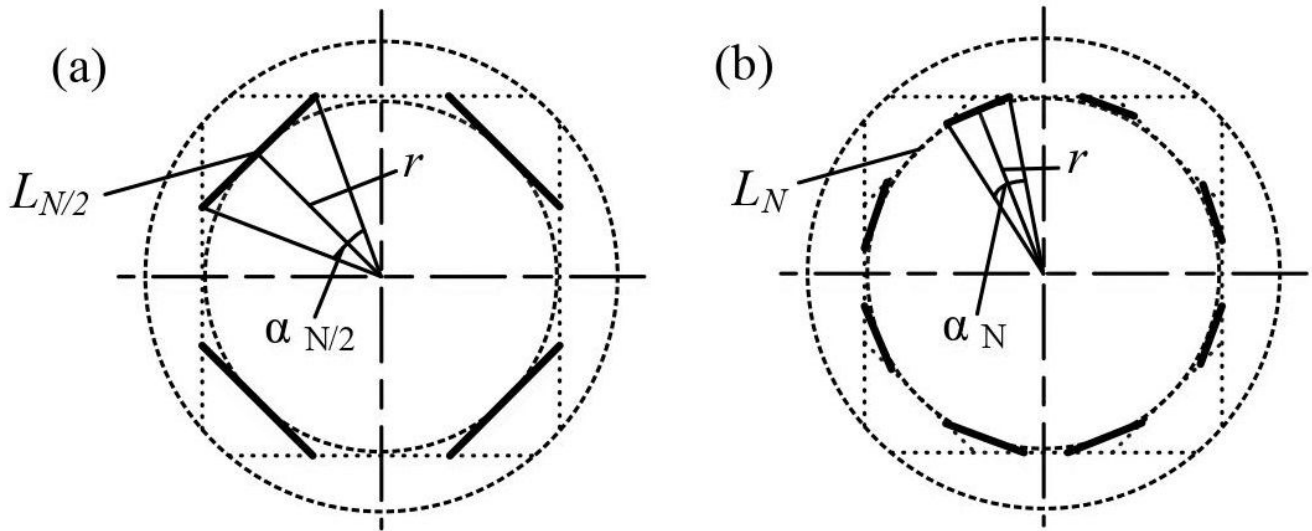


Figure 10

Cutting length calculation (a)  $L_{N/2}$  (b)  $L_N$

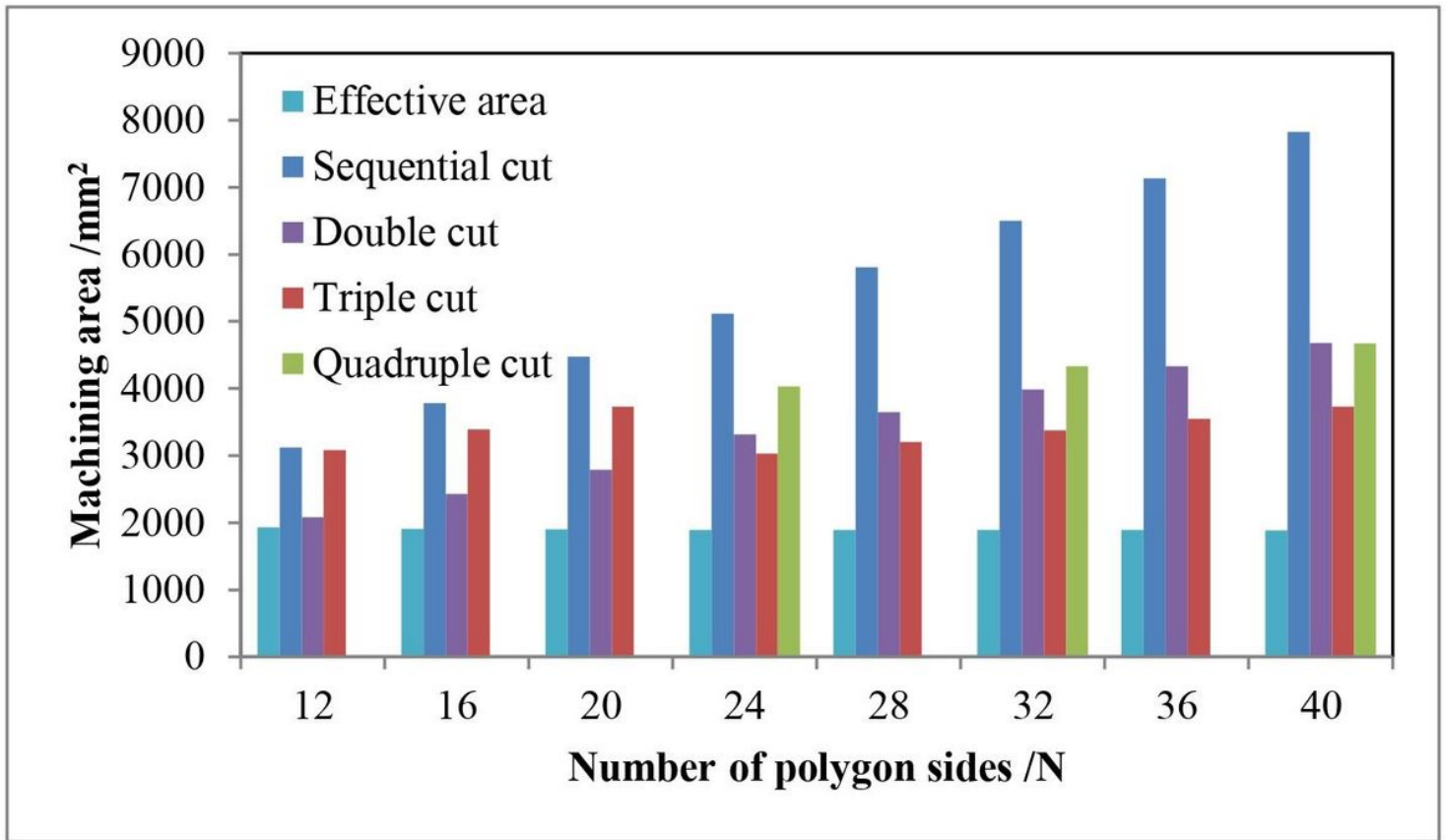


Figure 11

The relationship between the number of polygon sides and machining area

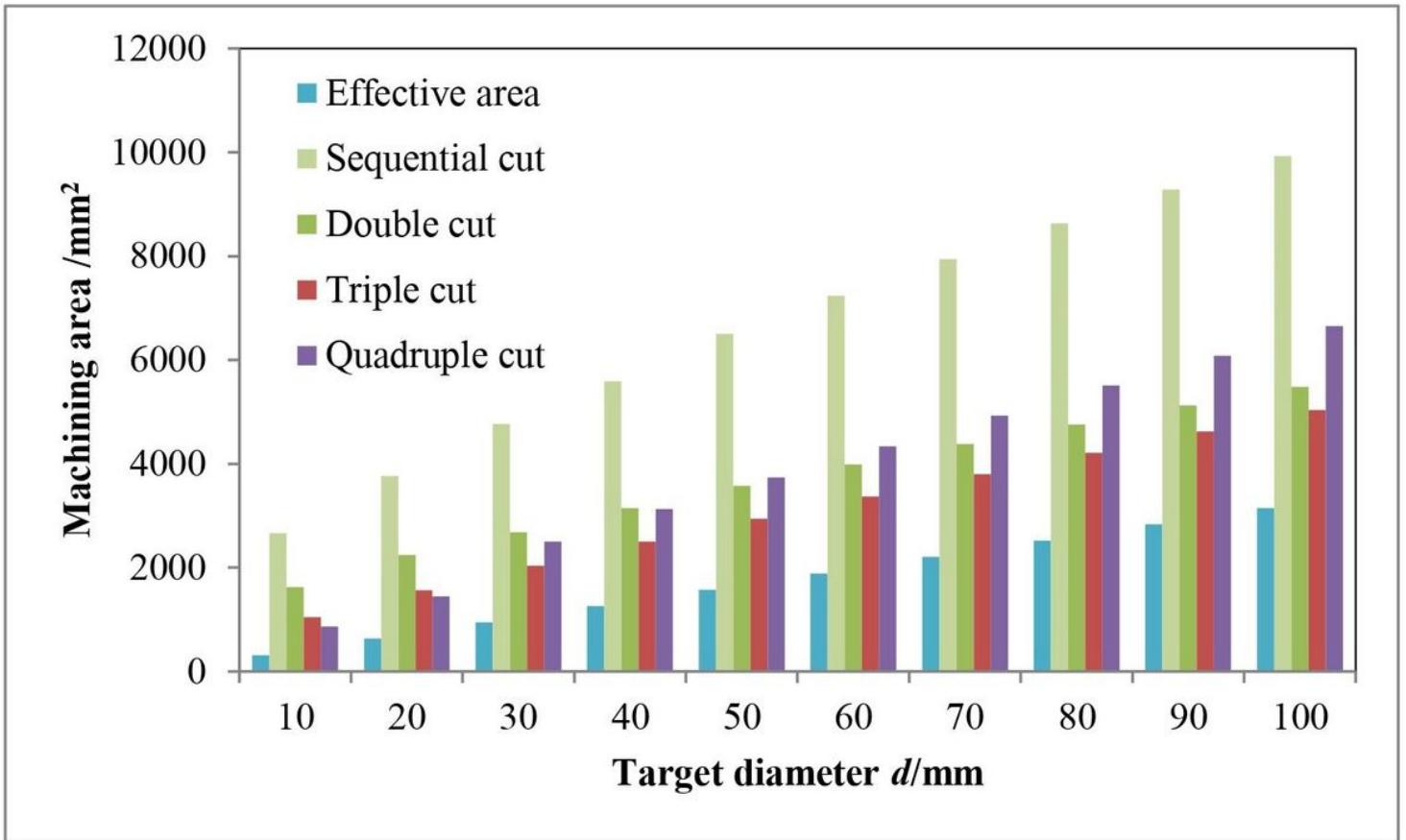


Figure 12

The influence of target size on machining area

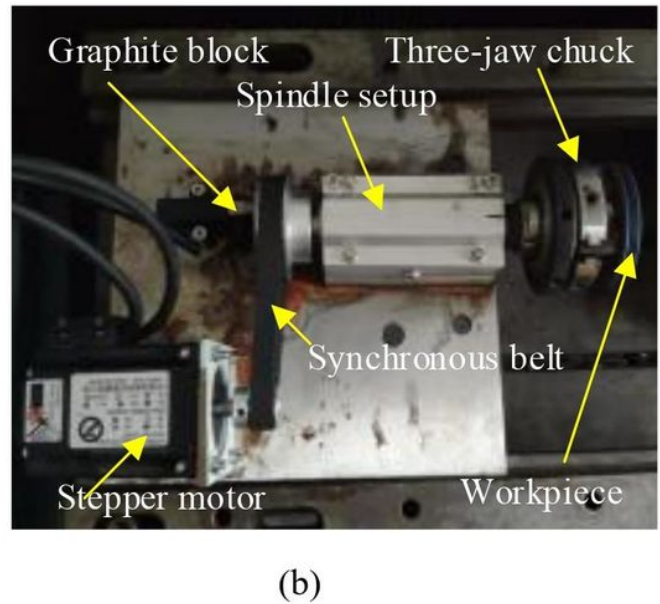
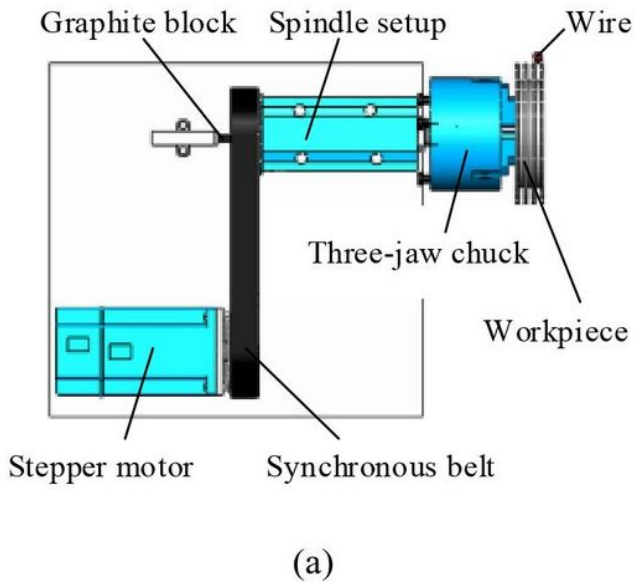


Figure 13

Cylindrical parts machining platform

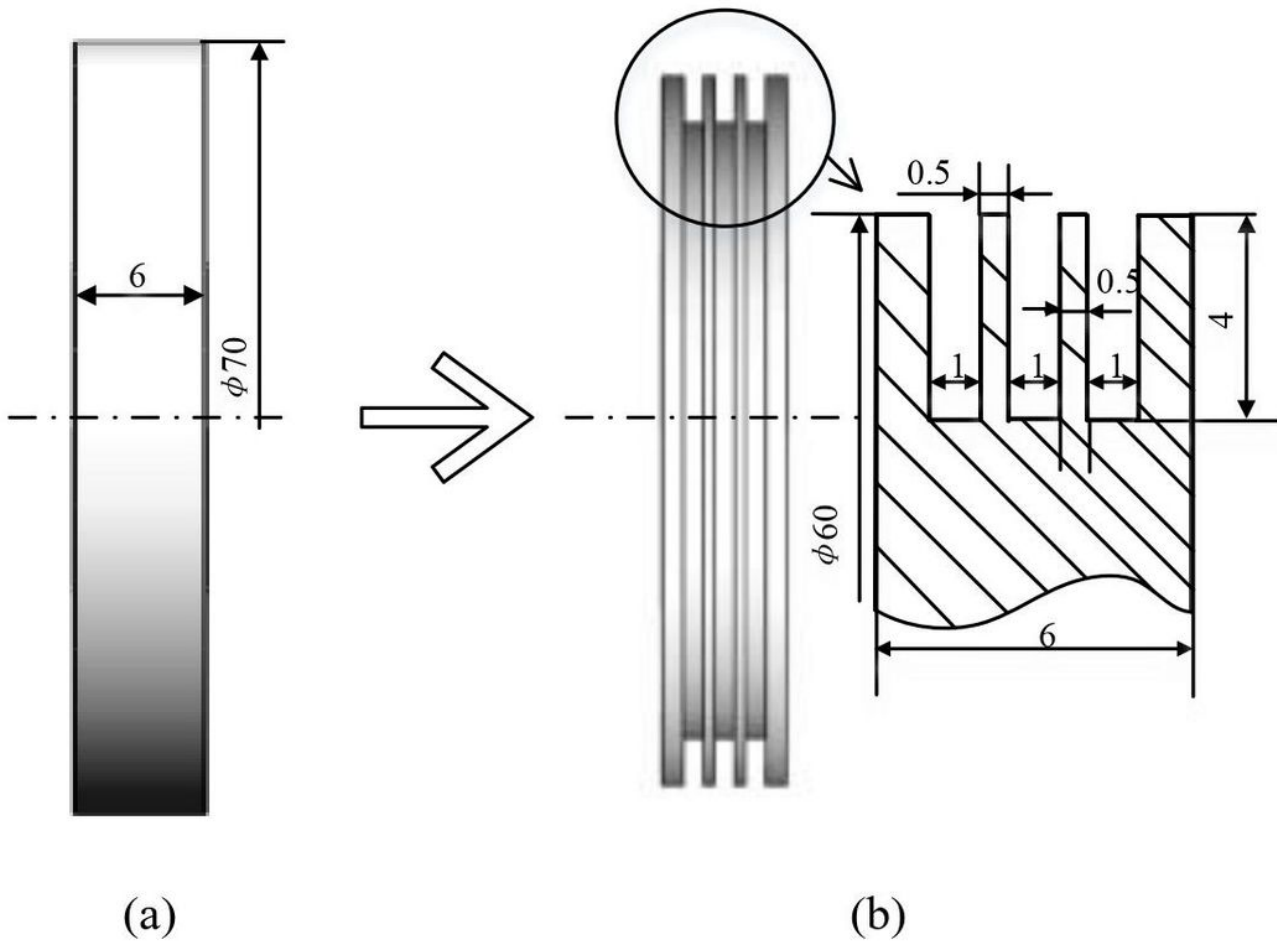


Figure 14

Dimensions of (a) raw part (b) processed part

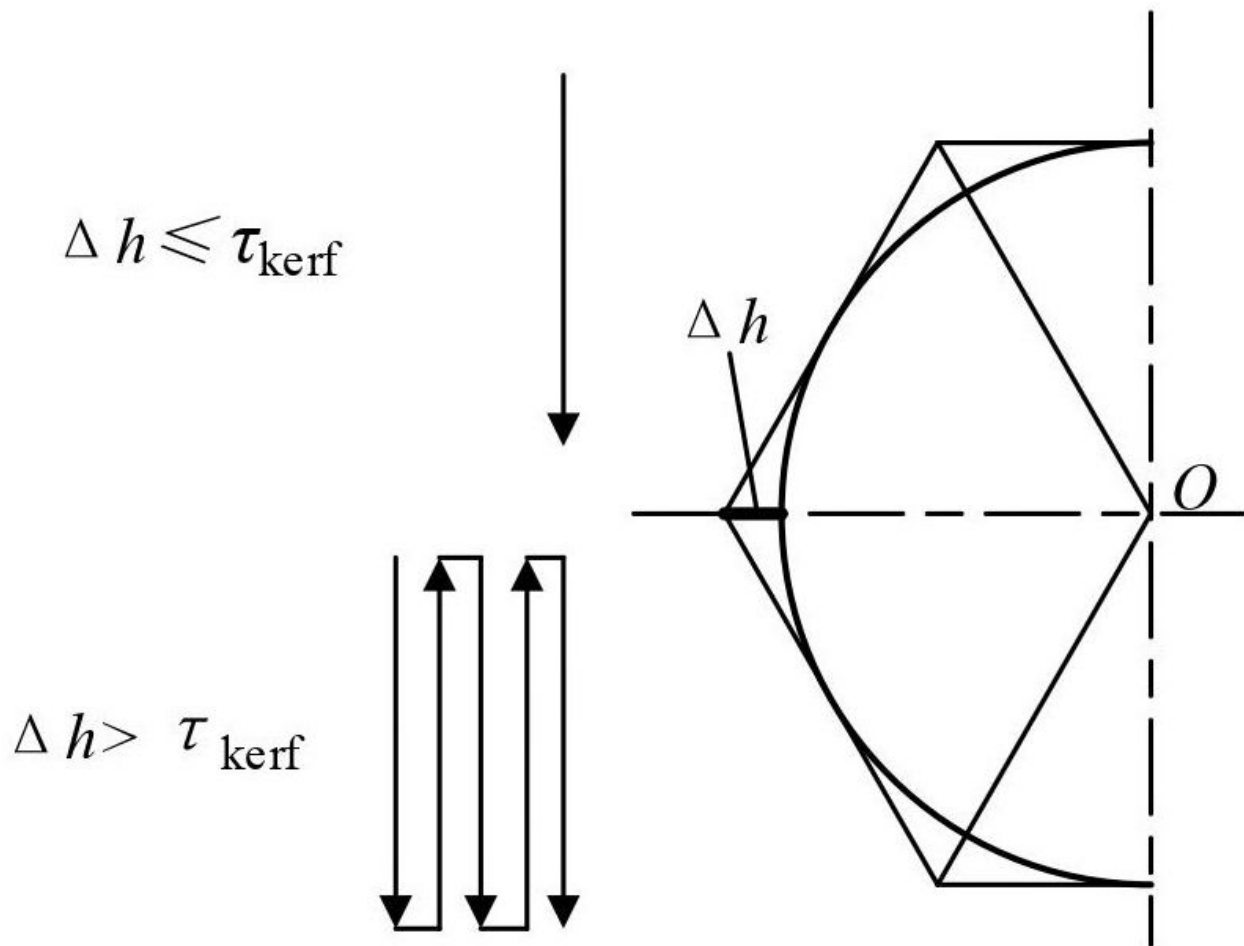
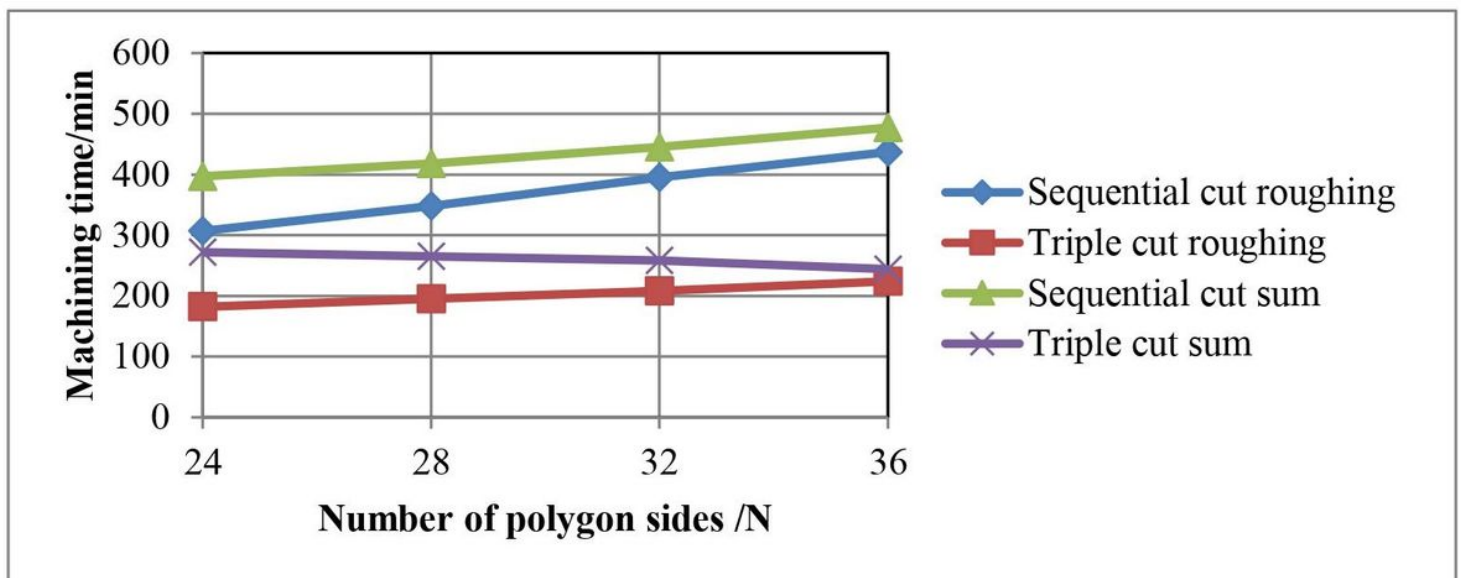


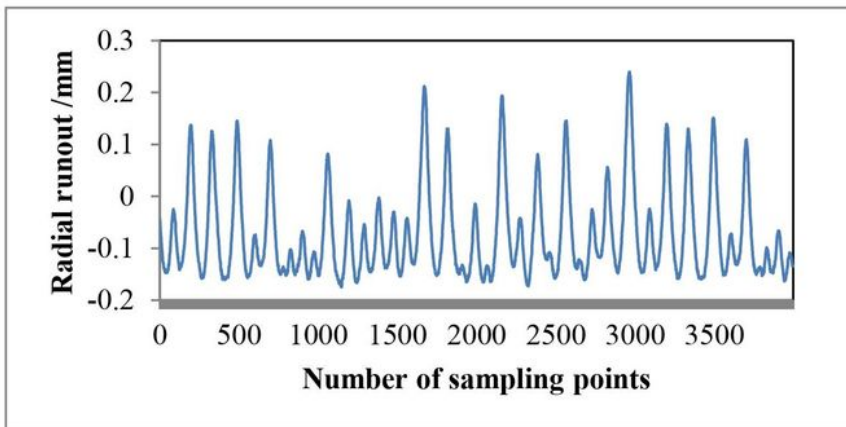
Figure 15

Countermeasures for residual height

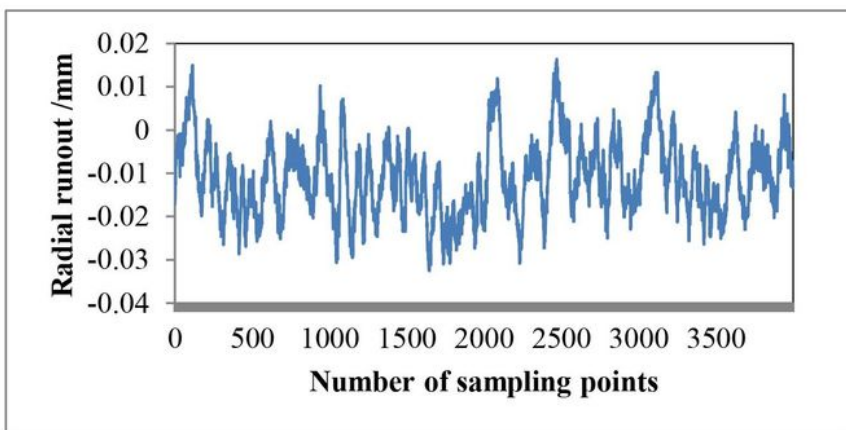


**Figure 16**

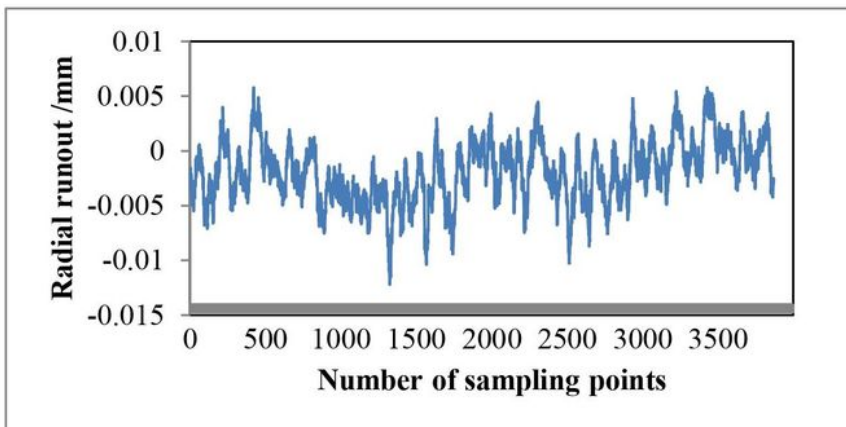
Machining time of two methods



(a)



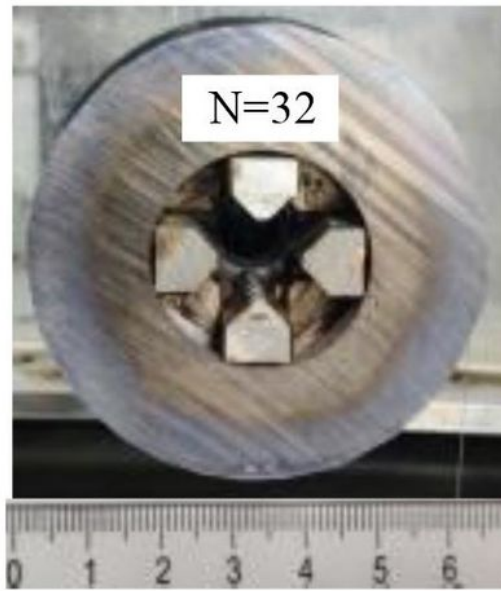
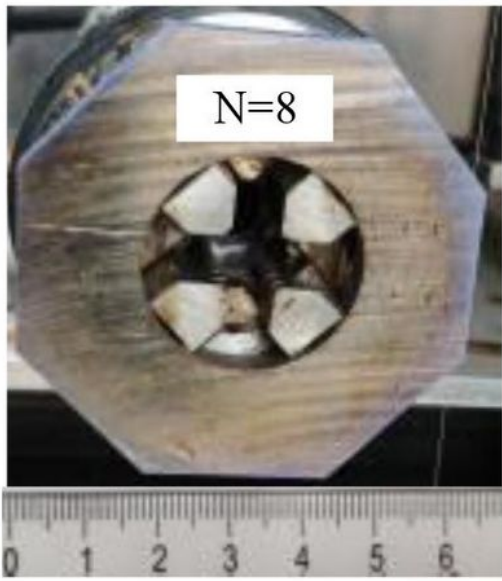
(b)



(c)

**Figure 17**

Data measurement in the circumferential direction (a) roughing (b) semi-finishing (c) finishing



(a)



(b)

**Figure 18**

Workpiece contour (a) online (b) completed